Structural Engineering and Mechanics, *Vol. 69, No. 3 (2019) 327-334*
DOI: https://doi.org/10.12989/sem.2019.69.3.327

Hygrothermal effects on the behavior of reinforced-concrete beams strengthened by bonded composite laminate plates

Kamel Antar*[1], Khaled Amara[2], Samir Benyoucef[1], Mokhtar Bouazza[3] and Mokhtar Ellali[2]

[1]*Material and Hydrology Laboratory, University of Sidi Bel Abbes, Faculty of Technology, Civil Engineering Department, 22000, Algeria*
[2]*Department of Civil Engineering, Faculty of Technology, University Center of Ain Temouchent, 46000, Algeria*
[3]*Department of Civil Engineering, Faculty of Technology, University of Bechar, 8000, Algeria*

(Received January 5, 2018, Revised January 2, 2019, Accepted January 9, 2019)

Abstract. The purpose of this paper is to investigate the hygrothermal effects on the behavior of reinforced-concrete beams strengthened by bonded composite laminate plates (θn/90 m)s. This work is based on a simple theoretical model to estimate the interfacial stresses developed between the concrete beam and the composite with taking into account the hygrothermal effect. Fibre orientation angle effects of number of 90° layers and effects of plate thickness and length on the distributions of interfacial stress in the concrete beams reinforced with composite plates have also been studied.

Keywords: interfacial stresses; concrete beam; composite laminate; hygrothermal effects; fibre angle

1. Introduction

The plate bonding technique is used to increase the strength and the stiffness or repair the existing reinforced concrete structure. The use of the composite fiber-reinforced plastic (FRP) become more and more very effective given its simplicity. Many studies have been conducted, to predict the interfacial stresses, see, for example, those by Tounsi *et al.* (2007), Tounsi (2006), Benyoucef *et al.* (2006), Vilnay (1988), Roberts (1989), Roberts *et al.* (1989), Malek *et al.* (1994), Robinovitch *et al.* (2000), Ye (2001), Smith *et al.* (2001), Barnes *et al.* (2001), Stratford *et al.* (2006). Bouazaoui (2008) have studied the interfacial shear strength between the steel bar surface and concrete surface of steel rods bonded into concrete. Many approximate closed-form solutions have been developed in the past decade for the interfacial stresses in beams bonded with a steel or FRP plate (Vilnay 1988, Roberts 1989, Roberts *et al.* 1989, Taljsten 1997, Smith *et al.* 2001, Tounsi 2006).

The solution presented by Smith *et al*. (2001) seems to be the more accurate widely applicable solution, particularly when the flexural stiffness of the bonded plate becomes significant. Rabinovich *et al.* (2000) has presented a higher order analysis in which the adhesive layer was treated as an elastic medium with negligible longitudinal stiffness. This leads to uniform stresses and linearly varying normal stresses through the thickness of the adhesive layer. The significance of their solution is that it is the first solution that satisfies the stress-free boundary condition at the ends of the adhesive layer. Using the same approach, they investigated the effects of an uneven adhesive layer Rabinovich *et al.* (2001) and material nonlinearity Rabinovich *et al.* (2001). Shen *et al.* (2001) proposed an alternative analytical complementary energy approach, which resulted in closed-form expressions. Recently, many authors have conducted a numerical study in different directions to illustrate the principal parameters in order to estimate the distributions of interfacial stress in beams reinforced with composite plates (Daouadji 2017, Bouakaz *et al.* 2014, Krour *et al.* 2014, Touati *et al.* 2015, Hadji *et al.* 2016, Kara 2016, Elamary *et al.* 2016). The analytical models present often the assumption of constant environment conditions, while the RC beam and the FRP are subjected to changing temperature and moisture conditions and it should be including in the analysis Gibson (1994). In this paper, the hygrothermal effects in the concrete beam and the soffit plate will be included to estimate the interfacial shear and normal stresses. For this case, we introduce an analytical solution which include the mechanical properties of the beam, the plate and the adhesive layer under thermal (temperature effect) and hygroscopic (moisture effect) conditions. The most used solution is Teng's solution Smith *et al.* (2001). This solution doesn't consider the fibre orientation contrary to Tounsi (2006) solution which will be used in this paper. The total interfacial stress is the sum of Tounsi solution and the additional one due to the hygrothermal deformation of the beam and the plate (Bouderba *et al.* 2013, Bousahla *et al*. 2016, Beldjelili *et al*. 2016, Menasria *et al.* 2017, Chikh *et al.* 2017).

We can use more advanced theory, for example, those by El-Haina *et al.* (2017), Younsi *et al.* (2018), Bouhadra *et al.* (2018), Benchohra *et al.* (2018), Bourada *et al.* (2018).

Results have been presented to show the hygro-thermal effect on the interfacial shear and normal stresses.

2. Theoretical modelling

*Corresponding author, Ph.D.
E-mail: antarkamel@gmail.com

http://www.techno-press.com/journals/sem&subpage=7
ISSN: 1225-4568 (Print), 1598-6217 (Online)

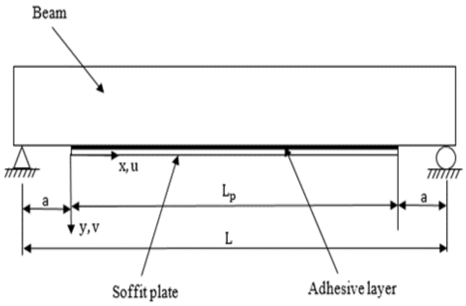

Fig. 1 Soffit-plated beam

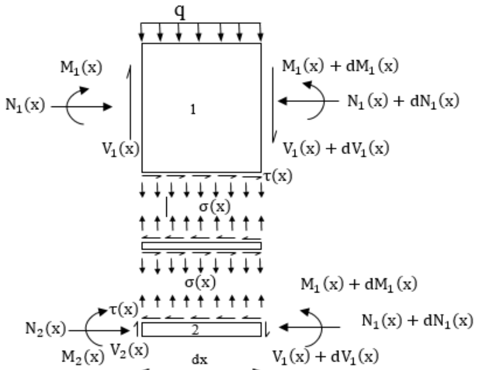

Fig. 2 Differential segment of a soffit-plated beam

As shown in Fig. 1, a concrete beam (Adherend 1) strengthened by FRP plate (Adherend 2) and bounded by an adhesive layer is considered. This beam is simply supported reinforced beam and subjected to a uniform distributed load. Geometry and cross-sections are shown in Fig. 1.

The following assumptions are used:

• The materials concrete beam, FRP plate and adhesive are linear elastic.

• Shear and normal stresses in the adhesive layer are constant across its thickness.

• The curvature in the beam and the plate are same.

2.1 Governing differential equations

The Fig. 2 represents a differential segment of plated beam. $\tau(x)$ and $\sigma(x)$ are the interfacial shear and normal stresses respectively with positive sign convention for the bending moment, shear force, axial force and applied loading. The derivation of the new solution below is described in terms of adherends 1 and 2, where adherend 1 is the beam and adherend 2 is the soffit plate.

The shear strain γ in the adhesive layer can be written as

$$\gamma = \frac{du(x,y)}{dy} + \frac{dv(x,y)}{dx} \tag{1}$$

$u(x,y)$ and $v(x,y)$ are the horizontal and vertical displacements of the adhesive layer respectively. $\tau(x)$ is given as

$$\tau(x) = G_a\left(\frac{du(x,y)}{dy} + \frac{dv(x,y)}{dx}\right) \tag{2}$$

where G_a is the shear modulus of the adhesive layer. Differentiating the expression (2) with respect to x gives

$$\frac{d\tau(x)}{dx} = G_a\left(\frac{d^2u(x,y)}{dy} + \frac{d^2v(x,y)}{dx}\right) \tag{3}$$

The curvature is function of the applied moment $M_T(x)$

$$\frac{d^2v(x)}{dx^2} = -\frac{1}{(EI)_t} M_T(x) \tag{4}$$

where $(EI)_t$ is the total flexural rigidity of the composite section. $u(x,y)$ must vary linearly across the adhesive thickness t_a, then

$$\frac{du}{dy} = \frac{1}{t_a}\left[u_2(x) - u_1(x)\right] \tag{5}$$

and

$$\frac{d^2u(x,y)}{dxdy} = \frac{1}{t_a}\left(\frac{du_2(x)}{dx} - \frac{du_1(x)}{dx}\right) \tag{6}$$

where $u_1(x)$ and $u_2(x)$ are the longitudinal displacements at the base of adherend 1 and the top of adherend 2, respectively. Eq. (3) can be rewritten as

$$\frac{d\tau(x)}{dx} = G_a\left(\frac{du_2(x)}{dx} - \frac{du_1(x)}{dx} - \frac{t_a}{(EI)_t} M_T(x)\right) \tag{7}$$

The third term in parentheses in Eq. (7) can be ignored Smith *et al.* (2001) in the following derivation. The strains at the base of adherend 1 and the top of adherend 2 taking account the hygrothermal deformations are given as

$$\varepsilon_1(x) = \frac{du_1(x)}{dx} = \frac{y_1}{E_1 I_1} M_1(x) - \frac{1}{E_1 A_1} N_1(x) + \alpha_1 \Delta T + \beta_1 \Delta C \tag{8}$$

Where α_1 is the coefficient of thermal expansion and β_1 is the coefficient of hygroscopic expansion of the RC beam. ΔT and ΔC are the temperature and percent moisture change respectively.

The laminate theory is used to estimate the strain of the symmetrical composite plate (Herakovich 1998), i.e.,

$$\varepsilon_x^0 = A'_{11} N_x \frac{1}{b_2} \quad \textit{and} \quad k_x = D'_{11} M_x \frac{1}{b_2} \tag{9}$$

$[A']$ is the inverse of the extensional matrix $[A]$; $[D']$ is the inverse of the flexural matrix $[D]$; b_2 is a width of FRP plate. Using CLT, the strain at the top of the FRP plate 2 is given as

$$\varepsilon_2(x) = \varepsilon_x^0 - k_x \frac{t_2}{2} + \alpha_2 \Delta T + \beta_2 \Delta C \tag{10}$$

Substituting Eqs. (9) in (10) gives the following equation

$$\varepsilon_2(x) = -D'_{11} \frac{t_2}{2b_2} M_2(x) + \frac{A'_{11}}{b_2} N_2(x) + \alpha_2 \Delta T + \beta_2 \Delta C \tag{11}$$

α_2 is the coefficient of thermal expansion and β_2 is the coefficient of hygroscopic expansion of the plate soffit.

Considering horizontal equilibrium gives

$$\frac{dN_1(x)}{dx} = \frac{dN_2(x)}{dx} = b_2\tau(x) \tag{12}$$

where

$$N_1(x) = N_2(x) = N(x) = b_2\int_0^x \tau(x)dx \tag{13}$$

The moments in the two adherends can be related as

$$M_1(x) = RM_2(x) \tag{14}$$

with

$$R = \frac{E_1 I_1}{E_2 I_2} \tag{15}$$

and the moment equilibrium of the differential segment of the plated beam in Fig. 2 gives

$$M_T(x) = M_1(x) + M_2(x) + N(x)(y_1 + y_2 + t_a) \tag{16}$$

The bending moment in each adherend is function of the total applied moment and the interfacial shear stress as

$$M_1(x) = \frac{R}{R+1}\left[M_T(x) - b_2\int_0^x \tau(x)(y_1 + y_2 + t_a)dx\right] \tag{17}$$

$$M_2(x) = \frac{1}{R+1}\left[M_T(x) - b_2\int_0^x \tau(x)(y_1 + y_2 + t_a)dx\right] \tag{18}$$

The first derivative of the bending moment in each adherend gives

$$\frac{dM_1(x)}{dx} = V_1(x) = \frac{R}{R+1}\left[V_T(x) - b_2\tau(x)(y_1 + y_2 + t_a)\right] \tag{19}$$

$$\frac{dM_2(x)}{dx} = V_2(x) = \frac{1}{R+1}\left[V_T(x) - b_2\tau(x)(y_1 + y_2 + t_a)\right] \tag{20}$$

Substituting Eqs. (8) and (11) into Eq. (7) and differentiating the resulting equation once yields

$$\frac{d^2\tau(x)}{dx^2} = \frac{G_a}{t_a}\left(\frac{-t_2}{2b_2}D'_{11}\frac{dM_2(x)}{dx} + \frac{A'_{11}}{b_2}\frac{dN_2(x)}{dx} - \frac{y_1}{E_1 I_1}\frac{dM_1(x)}{dx} + \frac{1}{E_1 A_1}\frac{dN_1(x)}{dx}\right) \tag{21}$$

Substitution of the shear forces (Eqs. (19) and (20)) and axial forces (Eq. (13)) in both adherends into Eq. (21) gives the following governing differential equation for the interfacial shear stress

$$\begin{aligned}&\frac{d^2\tau(x)}{dx^2} - \frac{G_a}{t_a}\left(A'_{11} + \frac{b_2}{E_1 I_1} + \frac{(y_1+y_2)(y_1+y_2+t_a)}{E_1 I_1 D'_{11} + b_2}b_2 D'_{11}\tau(x)\right)\\ &+ \frac{G_a}{t_a}\left(\frac{y_1+y_2}{E_1 I_1 D'_{11} + b_2}D'_{11}\right)V_T(x) = 0\end{aligned} \tag{22}$$

For simplicity and for such loading, $d_2V_T(x)/dx_2=0$, the general solution of Eq. (22) is given by

$$\tau(x) = B_1\cosh(\lambda x) + B_2\sinh(\lambda x) + m_1 V_T(x) \tag{23}$$

where

$$\lambda^2 = \frac{G_a}{t_a}\left(A'_{11} + \frac{b_2}{E_1 A_1} + \frac{(y_1+y_2)(y_1+y_2+t_a)}{E_1 I_1 D'_{11} + b_2}b_2 D'_{11}\right) \tag{24}$$

and

$$m_1 = \frac{G_a}{t_a\lambda^2}\left(\frac{y_1+y_2}{E_1 I_1 D'_{11} + b_2}D'_{11}\right) \tag{25}$$

The general solution for the interfacial shear stress for a simply supported beam subjected to a uniformly distributed load is given as

$$\tau(x) = B_1\cosh(\lambda x) + B_2\sinh(\lambda x) + m_1 q\left(\frac{L}{2} - x - a\right) \tag{26}$$

The constants of integration need to be determined by applying suitable boundary conditions.

At x=0, here the moment at the plate end $M_2(0)=N_1(0)=N_2(0)=0$ and as a result

$$M_1(0) = M_T(0) = \frac{qa}{2}(L-a) \tag{27}$$

Substituting Eqs. (8) and (11) into Eq. (7) with the third term ignored, and applying the above boundary condition, gives

$$\left.\frac{d\tau(x)}{dx}\right|_{x=0} = -m_2 M_T(0) \tag{28}$$

where

$$m_2 = \frac{G_a y_1}{t_a E_1 I_1} \tag{29}$$

By substituting Eq. (23) into Eq. (28), B2 can be determined as

$$\begin{aligned}B_2 &= -\frac{m_2 qa}{2\lambda}(L-a) + \frac{m_1}{\lambda}q + \\ &\frac{G_a}{t_a\lambda}\left[(\alpha_1 - \alpha_2)\Delta T + (\beta_1 - \beta_2)\Delta C\right] = -B_1\end{aligned} \tag{30}$$

The normal stress in the adhesive layer, $\sigma(x)$, is given as

$$\sigma(x) = \frac{E_a}{t_a}\left[v_2(x) - v_1(x)\right] \tag{31}$$

where $v_1(x)$ and $v_2(x)$ are the vertical displacements of adherend 1 and 2, respectively.

Differentiating Eq. (31) twice results in

$$\frac{d^2\sigma(x)}{dx^2} = K_n\left[\frac{d^2v_1(x)}{dx^2} - \frac{d^2v_2(x)}{dx^2}\right] \tag{32}$$

Considering the moment-curvature relationships for the beam to be strengthened and the external reinforcement, respectively

$$\frac{d^2v_1(x)}{dx^2}=\frac{M_1(x)}{E_1I_1}\frac{d^2v_2(x)}{dx^2}=-\frac{D_{11}^{'}M_2(x)}{dx^2} \tag{33}$$

The equilibrium of adherend 1 and 2, leads to the following relationships:

Adherend 1

$$\frac{dM_1(x)}{dx}=V_1(x)-b_2y_1\tau(x) \quad and \quad \frac{dV_1(x)}{dx}=-b_2y_1\sigma(x)-q \tag{34}$$

Adherend 2

$$\frac{dM_2(x)}{dx}=V_2(x)-b_2y_2\tau(x) \quad and \quad \frac{dV_2(x)}{dx}=-b_2\sigma(x) \tag{35}$$

Based on the above equilibrium equations, the governing differential equations for the deflection of adherends 1 and 2, expressed in terms of the interfacial shear and normal stresses, are given as follows:

Adherend 1

$$\frac{d^4v_1(x)}{dx^4}=-\frac{1}{E_1I_1}b_2\sigma(x)+\frac{y_1}{E_1I_1}b_2\frac{d\tau(x)}{dx}+\frac{q}{E_1I_1} \tag{36}$$

Adherend 2

$$\frac{d^4v_2(x)}{dx^4}=-D_{11}^{'}\sigma(x)+D_{11}^{'}y_2\frac{d\tau(x)}{dx}+\frac{q}{E_1I_1} \tag{37}$$

Substitution of Eqs. (36) and (37) into the fourth derivation of the interfacial normal stress obtainable from Eq. (31) gives the following governing differential equation for the interfacial normal stress

$$\frac{d^4\sigma(x)}{dx^4}+\frac{E_a}{t_a}\left(D_{11}^{'}+\frac{b_2}{E_1I_1}\right)\sigma(x) -\frac{E_a}{t_a}\left(D_{11}^{'}y_2-\frac{y_1b_2}{E_1I_1}\right)\frac{d\tau(x)}{dx}+\frac{qE_a}{t_aE_1I_1} \tag{38}$$

The general solution to this fourth-order differential equation is

$$\sigma(x)=e^{-\beta x}\left[C_1\cos(\beta x)+C_2\sin(\beta x)\right] +e^{-\beta x}\left[C_3\cos(\beta x)+C_4\sin(\beta x)\right] -n_1\frac{d\tau(x)}{dx}-n_2q \tag{39}$$

For large values of x it is assumed that the normal stress approaches zero, and as a result $C_3=C_4=0$. The general solution therefore becomes

$$\sigma(x)=e^{-\beta x}\left[C_1\cos(\beta x)+C_2\sin(\beta x)\right] +n_1\frac{d\tau(x)}{dx}-n_2q \tag{40}$$

where

$$\beta=\sqrt[4]{\frac{E_a}{4t_a}\left(\frac{b_2}{E_1I_1}+D_{11}^{'}\right)} \tag{41}$$

and

$$n_1=\frac{y_1b_2-D_{11}^{'}E_1I_1y_1}{D_{11}^{'}E_1I_1+b_2} \tag{42}$$

$$n_2=\frac{1}{D_{11}^{'}E_1I_1+b_2} \tag{43}$$

As is described by Smith *et al*. (2001), the constants C_1 and C_2 in Eq. (40) are determined using the appropriate boundary conditions

$$C_1=\frac{E_a}{2\beta^2t_a}\frac{1}{E_1I_1}\left[V_T(0)+\beta M_T(0)\right]-\frac{n_3}{2\beta^3}\tau(0) +\frac{n_1}{2\beta^3}\left(\left.\frac{d^4\tau(x)}{dx^4}\right|_{x=0}+\beta\left.\frac{d^3\tau(x)}{dx^3}\right|_{x=0}\right) \tag{44}$$

$$C_2=\frac{E_a}{2\beta^2t_a}\frac{1}{E_1I_1}M_T(0)-\frac{n_1}{2\beta^2}\left.\frac{d^3\tau(x)}{dx^3}\right|_{x=0} \tag{45}$$

where

$$n_3=\frac{E_ab_2}{t_a}\left(\frac{y_1}{E_1I_1}-\frac{D_{11}^{'}t_2}{2b_2}\right) \tag{46}$$

3. Results and discussion

Numerical results are presented to illustrate and examine both thermal and hygroscopic effects on the interfacial shear and normal stresses. We consider for this work an RC beam of 3000 mm of length, a soffit plate of L_P=2400 mm, a uniform distributed load q=50 KN/ml. The other geometric parameters and mechanicals properties are resumed in Table 1. All results are given for two cases of temperature and moisture change:

- ΔT=0°C, ΔC=0%
- ΔT=50°C, ΔC=1%

The hygrothermal properties used in this study are:

- $\alpha_1=11*10^{-6}$/°C and β_1= $*10^{-4}$(Edward G.N. (2008)),
- $\alpha_2=9*10^{-6}$/°C (Schmit 1998) and $\beta_2=1.89*10^{-3}$ (Vaddadi *et al.* 2007)

Figs. 3 to 12 shows the hygrothermal effect for various parameters. The maximum interfacial stresses increase

Table 1 Geometric and mechanicals properties

Component	Width (mm)	Depth (mm)	Young's Modulus (GPa)	Poisson's ratio
RC beam	200	300	30	
Soffit plate	200	4	50	
Adhesive layer	200	4	3	0.35

Table 2 Maximum interfacial shear and normal stresses

	τ_{max} (MPa)	σ_{max} (MPa)
Denton *et al.* (2001)	2.418	1.982
Deng *et al.* (2004)	2.410	2.007
Present $(0/90)_s$	2.959	1.392

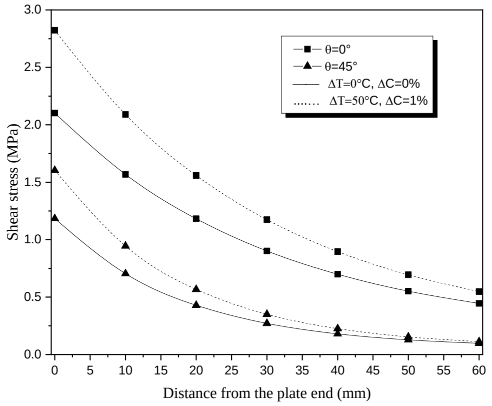

Fig. 3 Effect of fibre orientations on shear stress for an RC beam with a bonded composites laminates plate $[\theta/90]_s$ for different hygroscopic cases

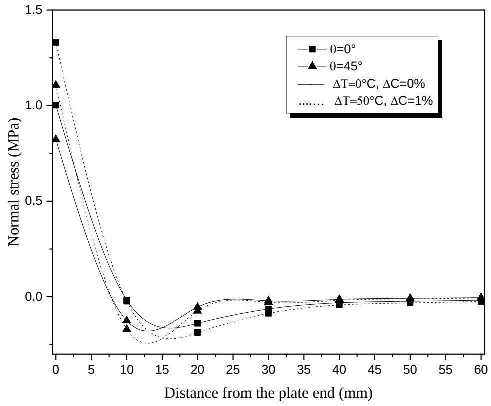

Fig. 4 Effect of fibre orientations on normal stress for an RC beam with a bonded composites laminates plate $[\theta/90]_s$ for different hygroscopic cases

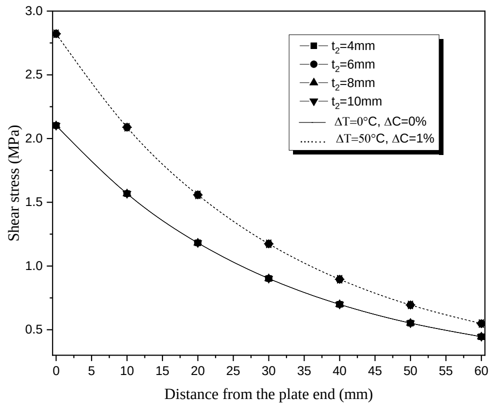

Fig. 5 Effect of plate thickness on shear stress for an RC beam with a bonded composites laminates plate $[0/90]_s$ under hygrothermal effect

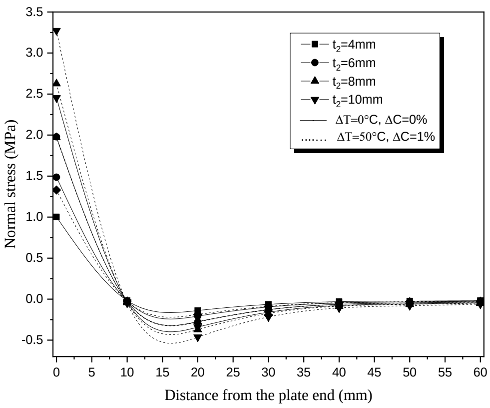

Fig. 6 Effect of plate thickness on normal stress for an RC beam with a bonded composites laminates plate $[0/90]_s$ under hygrothermal effect

considerably with considering the hygrothermal effect.

3.1 Comparison studies

In order to validate the accuracy of the present method, a comparison has been carried out with previously published results by Denton *et al.* (2001) and Deng *et al.* (2004) for ΔT=50°C. Comparison results of the maximum interfacial shear and normal stresses are shown in Tables 2. It can be observed a good agreement between the present study and those given by Denton *et al.* (2001) and Deng *et al.* (2004).

3.2 Fibre orientation

The fibre orientation affects significantly the development of interfacial stresses. It's shown in Figs. 3 and 4 that the shear and normal stresses decrease when the angle of orientation increases.

3.3 Plate thickness

Figs. 5 and 6 show the effects of the plate thickness on the interfacial stresses. It seen that this plate affects considerably the normal stress and hardly the shear stress concentration. The normal stress increase with increasing the plate thickness.

3.4 Adhesive layer thickness

It's shown in Figs. 7 and 8 that the level of interfacial stresses is influenced considerably by the thickness of the adhesive layer. The interface shear and normal stresses decrease with increasing the thickness of adhesive layer.

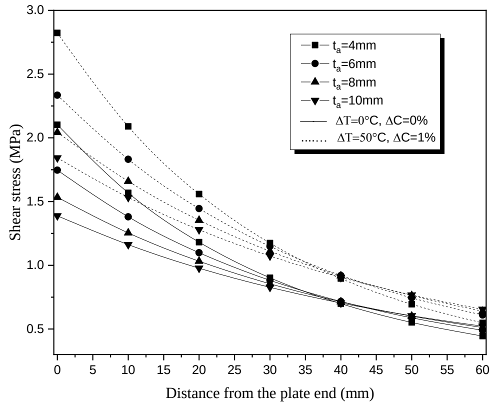

Fig. 7 Effect of adhesive layer thickness on shear stress for an RC beam with a bonded composites laminates plate $[0/90]_s$ under hygrothermal effect

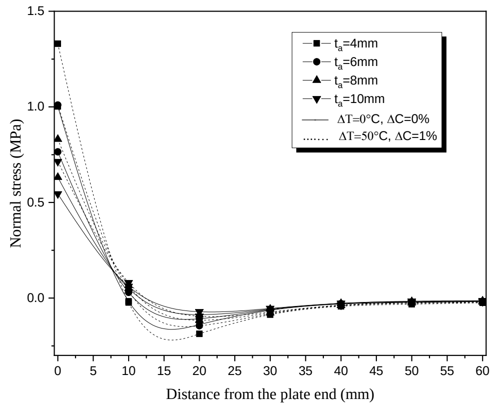

Fig. 8 Effect of adhesive layer thickness on normal stress for an RC beam with a bonded composites laminates plate $[0/90]_s$ under hygrothermal effect

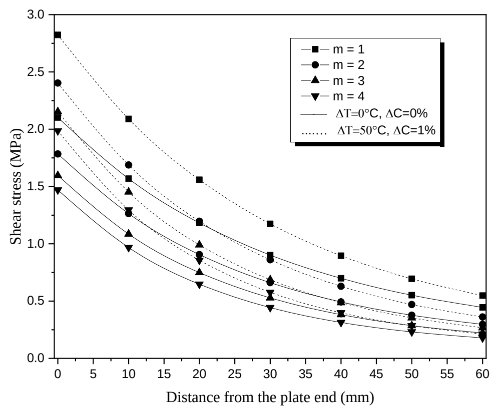

Fig. 9 Effect of external layer number on shear stress for an RC beam with a bonded composites laminates plate $[0/90_m]_s$ under hygrothermal effect

3.5 Number of laminate layers

The number of laminate layers have an important effect in the distribution of the interfacial stresses. Figs. 9 and 10 show a decreasing in both shear and normal stresses with increasing the number of external layers. On the other

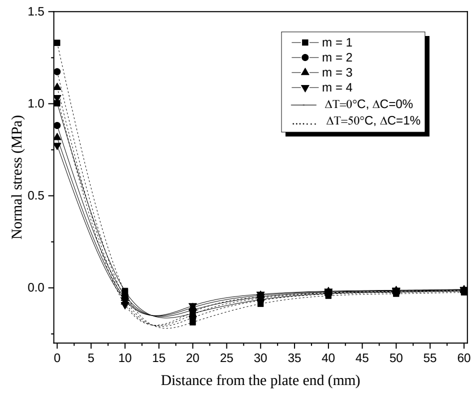

Fig. 10 Effect of external layer number on normal stress for an RC beam with a bonded composites laminates plate $[0/90_m]_s$ under hygrothermal effect

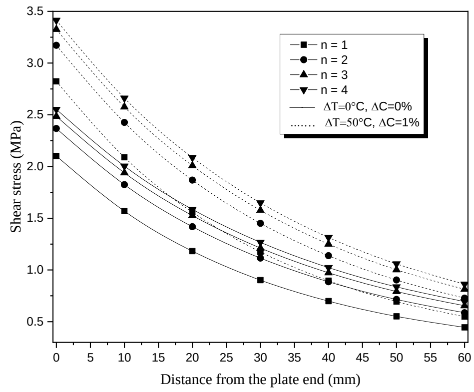

Fig. 11 Effect of internal layer number on shear stress for an RC beam with a bonded composites laminates plate $[0_n/90]_s$ under hygrothermal effect

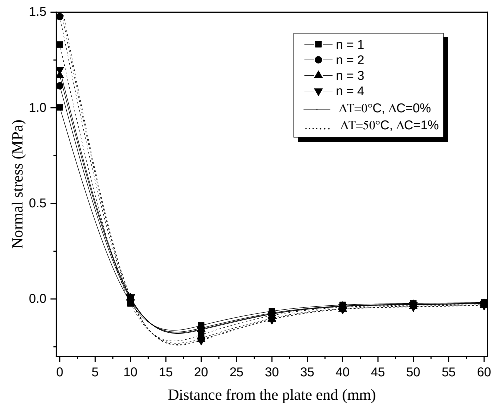

Fig. 12 Effect of internal layer number on normal stress for an RC beam with a bonded composites laminates plate $[0_n/90]_s$ under hygrothermal effect

hand, it's shown in Figs. 11 and 12 that normal and shear stresses increase when the number of internal layers increase.

4. Conclusions

A simple solution has been presented in this paper in order to calculate the interfacial stresses of retrofitted RC beam strengthened with a soffit plate under hygrothermal and mechanical loads with taking into account the fibre orientation. The following are the main conclusions.

• The inclusion of hygrothermal effect increases considerably the maximum interfacial shear and normal stresses.

• It's found that increasing the angle of fibre orientation reduces the interfacial stresses.

• The interfacial stresses increase with increasing the thickness of the FRP plate. No change has been found in the distribution of the shear stresses.

• Increasing the thickness of adhesive layer has a great role in the reduction of the interfacial shear and normal stresses.

• The interfacial stresses decrease with increasing the number of external layers and increases with increasing the number of internal layers.

Acknowledgments

The research described in this paper was supported by University centre of Ain Temouchent, University of Sidi Bel Abbes and University of Bechar in Algeria.

References

Barnes, R.A. and Mays, G.C. (2001), "The transfer of stress through a steel to concrete adhesive bond", *Int. J. Adhes.*, **21**(6), 495-502.

Beldjelili, Y., Tounsi, A. and Mahmoud, S.R. (2016), "Hygro-thermo-mechanical bending of S-FGM plates resting on variable elastic foundations using a four-variable trigonometricplate theory", *Smart Struct. Syst.*, **18**(4), 755-786.

Benachour, A., Benyoucef, S., Tounsi, A. and Adda Bedia, E A. (2008), "Interfacial stress analysis of steel beams reinforced with bonded prestressed FRP plate", *J. Eng. Struct.*, **30**(11), 3305-3315.

Benchohra, M., Driz, H., Bakora, A., Tounsi, A., Adda Bedia, E.A. and Mahmoud, S.R. (2018), "A new quasi-3D sinusoidal shear deformation theory for functionally graded plates", *Struct. Eng. Mech.*, **65**(1), 19-31.

Benyoucef, S., Tounsi, A., Meftah, S.A. and Adda Bedia, E.A. (2006), "Approximate analysis of the interfacial stress concentrations in FRP-RC hybrid beams", *Compos. Interf.*, **13**(7), 561-571.

Bouakaz, K., Hassaine Daouadji, T., Meftah, S.A., Ameur, M. and Adda Bedia, E.A. (2014), "A numerical analysis of steel beams strengthened with composite materials", *Mech. Compos. Mater.*, **50**(4), 685-696.

Bouazaoui, L.A. (2008), "Analysis of steel/concrete interfacial shear stress by means of pullout test", *Int. J. Adhes.*, **28**(3), 101-108.

Bouderba, B., Houari, M.S.A. and Tounsi, A. (2013), "Thermomechanical bending response of FGM thick plates resting on Winkler-Pasternak elastic foundations", *Steel Compos. Struct.*, **14**(1), 85-104.

Bouhadra, A., Tounsi, A., Bousahla, A.A., Benyoucef, S. and Mahmoud, S.R. (2018), "Improved HSDT accounting for effect of thickness stretching in advanced composite plates", *Struct. Eng. Mech.*, **66**(1), 61-73.

Bourada, F., Amara, K., Bousahla, A.A., Tounsi, A. and Mahmoud, S.R. (2018), "A novel refined plate theory for stability analysis of hybrid and symmetric S-FGM plates", *Struct. Eng. Mech.*, **68**(6), 661-675.

Bousahla, A.A., Benyoucef, S., Tounsi, A. and Mahmoud, S.R. (2016), "On thermal stability of plates with functionally graded coefficient of thermal expansion", *Struct. Eng. Mech.*, **60**(2), 313-335.

Chikh, A., Tounsi, A., Hebali, H. and Mahmoud, S.R. (2017), "Thermal buckling analysis of cross-ply laminated plates using a simplified HSDT", *Smart Struct. Syst.*, **19**(3), 289-297.

Deng, J. and Marcus, M.K. (2004), "Stress analysis of steel beams reinforced with a bonded CFRP plate", *Compos. Struct.*, **65**(2), 205-215.

Denton, S.N. (2001), "Analysis of stresses developed in FRP plated beams due to thermal effects", *FRP Compos. Civil Eng.*, 527-536.

Edward, G.N. (2008), *Concrete Construction Engineering Handbook*, CRC Press.

El-Haina, F., Bakora, A., Bousahla, A.A., Tounsi, A. and Mahmoud, S.R. (2017), "A simple analytical approach for thermal buckling of thick functionally graded sandwich plates", *Struct. Eng. Mech.*, **63**(5), 585-595.

Elamary, A.S. and Abd-Elwahab, R.K. (2016), "Numerical simulation of concrete beams reinforced with composite GFRP-Steel bars under three points bending" *Struct. Eng. Mech.*, **57**(5), 937-949.

Gibson, R.F. (1994), *Principles of Composites Material Mechanics*, McGraw-Hill Inc.

Hadji, L., Hassaine Daouadji, T., Meziane, A.M. and Adda Bedia, E.A. (2016), "Analyze of the interfacial stress in reinforced concrete beams strengthened with externally bonded CFRP plate", *Steel Compos. Struct.*, **20**(2), 413-429.

Hassaine Daouadji, T. (2017), "Analytical and numerical modeling of interfacial stresses in beams bonded with a thin plate", *Adv. Comput. Des.*, **2**(1), 57-69.

Herakovich, CT. (1998), *Mechanics of Fibrous Composites*, Wiley, U.S.A.

Kara, I.F. (2016), "Flexural performance of FRP-reinforced concrete encased steel composite beams", *Struct. Eng. Mech.*, **59**(4), 775-793.

Krour, B., Bernard, F. and Tounsi, A. (2014), "Fibers orientation optimization for concrete beam strengthened with a CFRP bonded plate: A coupled analytical-numerical investigation", *Eng. Struct.*, **56**, 218-227.

Malek, A.M., Saadatmanesh, H. and Ehsani, M.R. (1998), "Prediction of failure load of RC beams strengthened with FRP plate due to stress concentration at the plate end", *ACI Struct. J.*, **95**(1), 142-152.

Menasria, A., Bouhadra, A., Tounsi, A., Bousahla, A.A. and Mahmoud, S.R. (2017), "A new and simple HSDT for thermal stability analysis of FG sandwich plates", *Steel Compos. Struct.*, **25**(2), 157-175.

Roberts, TM. (1989), "Approximate analysis of shear and normal stress concentrations in the adhesive layer of plated RC beams", *Struct. Eng.*, **67**(12), 229-233.

Roberts, TM. and Haji-Kazemi, H. (1989), "Theoretical study of the behavior of reinforced concrete beams strengthened by externally bonded steel plates", *Proc. Inst. Civil Eng.*, **87**(2), 39-55.

Robinovitch, O. and Frostig, Y. (2000), "Closed-form higher-order analysis of beams strengthened with FRP strips", *J. Compos. Constr.*, **4**(2), 65-74.

Robinovitch, O. and Frostig, Y. (2001), "Nonlinear higher-order analysis of cracked RC beams strengthened with FRP strips", *J. Struct. Eng.*, **127**(4), 381-389.

Schmit, K. (1998), *Fiberglass Reinforced Plastic (FRP) Piping Systems Designing Process/Facilities Piping Systems with FRP* *a Comparison to Traditional Metallic Materials*, Project Engineer Specialty Plastics, Inc. Baton Rouge, LA, U.S.A.

Shen, H.S., Teng, J.G. and Yang, J. (2001), “Interfacial stresses in beams and slabs bonded with a thin plate”, *J. Eng. Mech.*, **127**(4), 399-406.

Smith, S.T. and Teng, J.G. (2001), “Interfacial stresses in plated beams”, *Eng. Struct.*, **23**(7), 857-871.

Smith, S.T. and Teng, J.G. (2002), “FRP-strengthened RC beams. I: Review of debonding strength models”, *Eng. Struct.*, **24**(4), 385-395.

Smith, S.T. and Teng, J.G. (2002), “FRP-strengthened RC beams. II: Assessment of debonding strength models”, *Eng. Struct.*, **24**(4), 397-417.

Stratford, T. and Cadei, J. (2006), “Elastic analysis of adhesion stresses for the design of a strengthened plate bonded to a beam”, *Constr. Build. Mater.*, **20**(1-2), 34-45.

Taljsten, B. (1997), “Strengthening of beams by plate bonding”, *J. Mater. Civil Eng.*, **9**(4), 206-212.

Touati, M., Tounsi, A. and Benguediab, M. (2015), “Effect of shear deformation on adhesive stresses in plated concrete beams: Analytical solutions”, *Comput. Concrete*, **15**(3), 141-166.

Tounsi, A. and Benyoucef, S. (2007), “Interfacial stresses in externally FRP-plated concrete beams”, *Int. J. Adhes. Adhes.*, **27**(3), 207-215.

Tounsi, A. (2006), “Improved theoretical solution for interfacial stresses in concrete beams strengthened with FRP plate”, *Int. J. Sol. Struct.*, **43**(14-15), 4154-4174.

Vaddadi, P., Nakamura, T. and Singh, R.P. (2007), “Inverse analysis to determine hygrothermal properties in fiber reinforced composites”, *J. Compos. Mater.*, **41**(3), 309-344.

Vilnay, O. (1988), “The analysis of reinforced concrete beams strengthened by epoxy bonded steel plates”, *Int. J. Cement Compos. Light Weight Concrete*, **10**(2), 73-78.

Ye, J.Q. (2001), “Interfacial shear stress transfer of RC beams strengthened by bonded composite plates”, *Cement Concrete Compos.*, **23**(4-5), 411-417.

Younsi, A., Tounsi, A., Zaoui, F.Z., Bousahla, A.A. and Mahmoud, S.R. (2018), “Novel quasi-3D and 2D shear deformation theories for bending and free vibration analysis of FGM plates”, *Geomech. Eng.*, **14**(6), 519-532.

CC